Acta Crystallographica Section B
Structural Science
ISSN 0108-7681

Experimental and predicted crystal structures of Pigment Red 168 and other dihalogenated anthanthrones

Martin U. Schmidt,[a]* Erich F. Paulus,[b] Nadine Rademacher[a,b] and Graeme M. Day[c]

[a]Institut für Anorganische und Analytische Chemie, Goethe-Universität Frankfurt, Max-von-Laue-Strasse 7, D-60348 Frankfurt am Main, Germany, [b]Institut für Geowissenschaften, FE Mineralogie, Abt. Kristallographie, Goethe-Universität Frankfurt, Altenhöferallee 1, D-60438 Frankfurt am Main, Germany, and [c]Department of Chemistry, University of Cambridge, Lensfield Road, Cambridge CB2 1EW, England

Correspondence e-mail: m.schmidt@chemie.uni-frankfurt.de

Received 1 March 2010
Accepted 14 July 2010

The crystal structures of 4,10-dibromo-anthanthrone (Pigment Red 168; 4,10-dibromo-dibenzo[*def*,*mno*]chrysene-6,12-dione), 4,10-dichloro- and 4,10-diiodo-anthanthrone have been determined by single-crystal X-ray analyses. The dibromo and diiodo derivatives crystallize in $P2_1/c$, $Z = 2$, the dichloro derivative in $P\bar{1}$, $Z = 1$. The molecular structures are almost identical and the unit-cell parameters show some similarities for all three compounds, but the crystal structures are neither isotypic to another nor to the unsubstituted anthanthrone, which crystallizes in $P2_1/c$, $Z = 8$. In order to explain why the four anthanthrone derivatives have four different crystal structures, lattice-energy minimizations were performed using anisotropic atom–atom model potentials as well as using the semi-classical density sums (SCDS-Pixel) approach. The calculations showed the crystal structures of the dichloro and the diiodo derivatives to be the most stable ones for the corresponding compound; whereas for dibromo-anthanthrone the calculations suggest that the dichloro and diiodo structure types should be more stable than the experimentally observed structure. An experimental search for new polymorphs of dibromo-anthanthrone was carried out, but the experiments were hampered by the remarkable insolubility of the compound. A metastable nanocrystalline second polymorph of the dibromo derivative does exist, but it is not isostructural to the dichloro or diiodo compound. In order to determine the crystal structure of this phase, crystal structure predictions were performed in various space groups, using anisotropic atom–atom potentials. For all low-energy structures, X-ray powder patterns were calculated and compared with the experimental diagram, which consisted of a few broad lines only. It turned out that the crystallinity of this phase was not sufficient to determine which of the calculated structures corresponds to the actual structure of this nanocrystalline polymorph.

1. Introduction

4,10-Dibromo-anthanthrone [(2), see Fig. 1] has been industrially produced for more than 80 years. The pigment, having a reddish orange colour, is registered as Pigment Red 168 and used, *e.g.*, for automotive coatings. The dichloro derivative is yellow, whereas the diiodo derivative is wine-red. The dibromo derivative is even mentioned in standard textbooks on organic chemistry, *e.g.* in Fieser & Fieser (1957).

The X-ray powder diffraction diagrams of the dichloro-, dibromo- and diiodo-anthanthrones [(1)–(3)] are quite different, indicating that the three crystal structures are different, although the molecular structures are quite similar. We determined the crystal structures of (1)–(3) by X-ray structure analyses. The crystallographic similarities and

© 2010 International Union of Crystallography
Printed in Singapore – all rights reserved

dissimilarities will be shown, as well as a comparison with the crystal structure of unsubstituted anthanthrone (4), whose crystal structure was determined in 1971 (Edwards & Stadler, 1971).

In order to explain why the four anthanthrone derivatives (1)–(4) have four different crystal structures, we performed lattice-energy minimizations using anisotropic atom–atom model potentials as well as lattice-energy calculations with the semi-classical density sums (SCDS-Pixel) approach (Gavezzotti, 2003*a*,*b*).

The diiodo-anthanthrone (3) was one of the test compounds for the third blind test of crystal structure prediction organized by the Cambridge Crystallographic Data Centre in 2004 (Day *et al.*, 2005). The results of the blind test showed the importance of anisotropic atom–atom potentials in modelling interactions involving the I atoms.

1.1. History, synthesis and application

Anthanthrone (4) was first synthesized in 1912 or 1913 by Ludwig Kalb from 'Chemisches Laboratorium der Königlichen Akademie der Wissenschaften zu München' (Chemical Laboratory of the Royal Academy of Sciences in Munich, Germany). He synthesized 1,1′-binaphthyl-8,8′-dicarboxylic acid (5) and treated its diethyl ester with concentrated sulfuric acid at *ca* 373 K (see Fig. 2). A green solution of protonated anthanthrone is produced, which is poured onto water to give the orange–yellow anthanthrone (4). To prove the constitution of the product, the synthesis was repeated starting from 1,1′-binaphthyl-2,2′-dicarboxylic acid (6), which gave the same product. Since the product can be regarded as an annellation of two molecules of anthrone, he called it 'anthanthrone' (Kalb, 1914). Dibromo-anthanthrone (2) is synthesized either by bromination of (5) and subsequent ring closure with H_2SO_4 or – more easily – in a one-step procedure by adding Br_2 at the start of the treatment of (5) in concentrated H_2SO_4. Alternatively it can be synthesized by bromination of anthanthrone with Br_2 at 543–553 K (Kalb, 1913*b*).

On 26 March 1913 Kalb applied for a patent which describes syntheses and applications of anthanthrone and its substituted derivatives, including the dibromo derivative (2) (Kalb, 1913*a*). A few months later he applied for a second patent (Kalb, 1913*b*). Subsequently, Kalb seems to have contacted BASF. There he learned that the BASF chemists Dr Lüttringhaus and Dr Braren had developed a new unpublished synthetic route to the starting material (6); this route was much easier than Kalb's own synthesis for (6). BASF supplied him with information and samples. On 13 May 1914 Kalb submitted a publication on his results; BASF even allowed him to include a detailed description of their new procedure for the synthesis of (6) (Kalb, 1914).

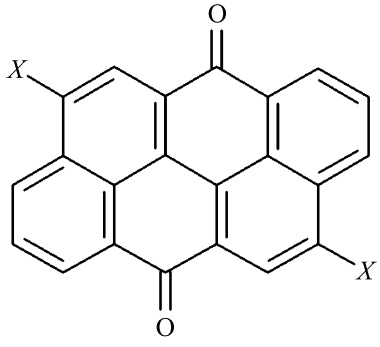

(1): X = Cl

(2): X = Br

(3): X = I

(4): X = H

Figure 1
Molecular formula of the anthanthrones.

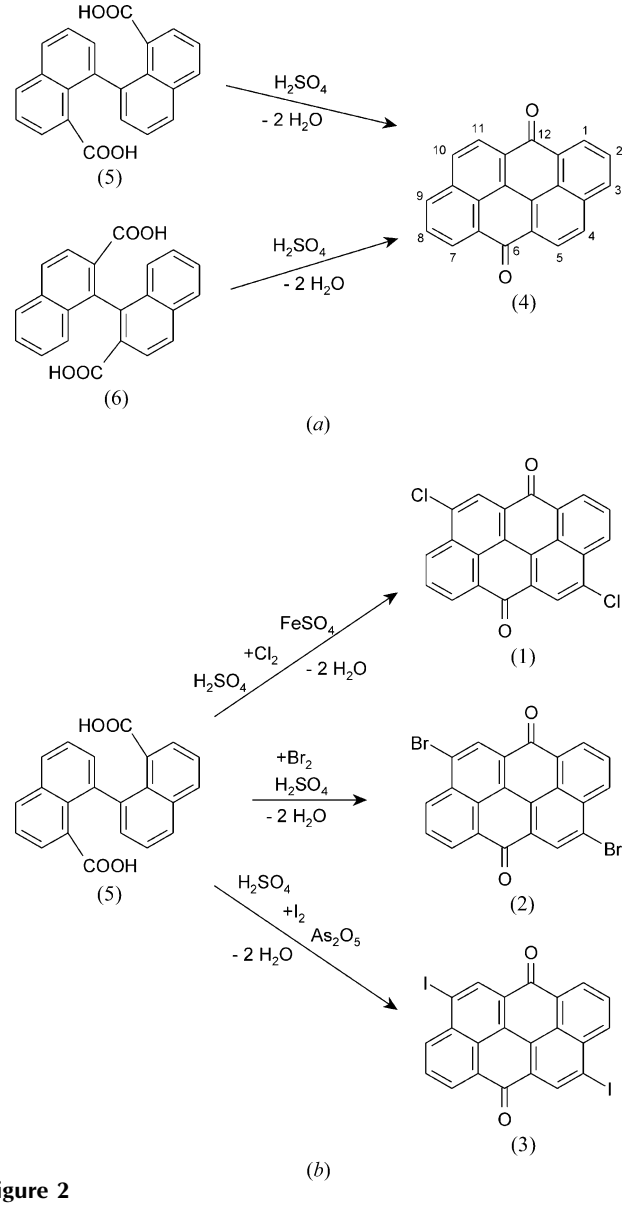

Figure 2
Top: syntheses of anthanthrone. The atom-numbering scheme in anthanthrone is also indicated. Bottom: syntheses of substituted anthanthrones.

Table 1
Crystal data and structure refinements.

Experiments were carried out at 293 K with Mo $K\alpha$ radiation using a R3m/V (Siemens) diffractometer. Refinement was without restraints.

Compound	(1) X = Cl	(2) X = Br	(3) X = I
Crystal data			
Chemical formula	$C_{22}H_8Cl_2O_2$	$C_{22}H_8Br_2O_2$	$C_{22}H_8I_2O_2$
M_r	375.18	464.10	558.08
Crystal system, space group	Triclinic, $P\bar{1}$	Monoclinic, $P2_1/c$	Monoclinic, $P2_1/c$
a, b, c (Å)	3.795 (1), 9.527 (1), 10.662 (1)	3.865 (1), 19.424 (2), 10.113 (1)	4.202 (1), 20.956 (4), 9.276 (2)
α, β, γ (°)	105.78 (1), 93.27 (1), 95.26 (1)	90, 92.56 (1), 90	90, 100.63 (3), 90
V (Å^3)	368.04 (11)	758.5 (2)	802.8 (3)
Z	1	2	2
Molecular site symmetry	$\bar{1}$	$\bar{1}$	$\bar{1}$
μ (mm^{-1})	0.46	5.36	3.93
Crystal size (mm)	0.51 × 0.05 × 0.02	0.5 × 0.25 × 0.01	0.38 × 0.08 × 0.04
Data collection			
Absorption correction	ψ scan	ψ scan	ψ scan
T_{min}, T_{max}	0.973, 0.991	0.218, 0.948	0.278, 0.337
No. of measured, independent and observed [$I > 2\sigma(I)$] reflections	3548, 1774, 842	3661, 1838, 1499	3914, 1965, 1277
R_{int}	0.091	0.026	0.080
Refinement			
$R[F^2 > 2\sigma(F^2)]$, $wR(F^2)$, S	0.071, 0.178, 0.93	0.044, 0.118, 1.04	0.042, 0.099, 0.98
No. of reflections	1774	1838	1965
No. of parameters	134	134	118
$\Delta\rho_{max}$, $\Delta\rho_{min}$ (e Å^{-3})	0.40, −0.45	0.55, −0.58	0.78, −0.62

Computer programs: *R3m/V* software (Siemens, 1989), *SHELXS*97, *SHELXL*97, *SHELXTL-Plus*97 (Sheldrick, 2008).

Finally the anthanthrones were produced not by BASF, but by Farbwerke Höchst, vorm. Meister Lucius & Brüning (later named Hoechst AG). The production of the dibromo derivative started in 1926 and of the dichloro derivative in 1928 (Formánek & Knop, 1927; Schultz, 1934). The products were sold as 'Indanthrenbrillantorange RK®' and 'Indanthrenbrillantorange GK®'. An improved procedure for the bromination of anthanthrone was developed, using iodine as a catalyst and SO_3 as an oxidizing agent to oxidize the HBr back to Br_2 and thus minimize the waste of bromine (Herz & Zerweck, 1932).

Initially the dibromo-anthanthrone was believed to be the 2,8-dibromo isomer (see *e.g.* Schaeffer, 1951). In 1953, *i.e.* 40 years after the first syntheses, the product was found not to be the 2,8 but the 4,10 isomer (Maki & Hashimoto, 1953; Bradley & Waller, 1953), *i.e.* for more than 25 years the pigments were produced and sold under the wrong structural formula!

Dibromo-anthanthrone was initially only used as a vat dye, like indigo. In this procedure the pigment is treated *e.g.* with $NaHSO_3$ in diluted NaOH. The C═O groups are thereby reduced to hydroxy groups, and the pigment becomes soluble. The resulting violet solution is used to dye cotton. Re-oxidation takes place in air which fixes the dibromo-anthanthrone on the cotton fibers. The resulting colour is described by Kalb as 'ein feuriges Rot' (a fiery red). The dichloro derivative is more yellowish, whereas the diiodo derivative exhibits a wine-red colour.

The parent compound (4) has no commercial value due to its low colour strength (Schweizer, 1964).

The diiodo derivative (3) was industrially produced from anthanthrone with I_2 in H_2SO_4 using arsenic pentoxide (!) as an oxidant. The product was sold as 'Indanthrene Scarlet FR®'. When dibromo-anthanthrone was present during the synthesis, a mixed bromo-iodo-anthanthrone was obtained (FIAT report, 1948, p. 95), which was sold as 'Vat Scarlet RM'. Acccording to mass spectroscopy this product did not actually contain 4-bromo-10-iodo-anthanthrone, but consisted of a mixture of 4,10-dibromo- and 4,10-diiodo-anthanthrone (Mix, 1986). The production of both diiodo products has long since been abandoned because of ecological problems (As_2O_3 in the waste water).

Today, only dibromo-anthanthrone is produced. It is still synthesized from 1,1′-binaphthyl-8,8′-dicarboxylic acid (5) with Br_2 in concentrated sulfuric acid. The resulting crude product is still sold as 'Indanthrene Brilliant Orange RK ®', and used as a vat dye (Vat Orange 3). Additionally, the product is transformed to a pigmentary form by a finishing procedure. This finishing can be done *e.g.* by dissolving the crude product in 100% H_2SO_4, and subsequently diluting the solution with 85% H_2SO_4, which causes the pigment to precipitate as oxonium sulfate (FIAT report, 1948). Final hydrolysis with water gives the compound in pigmentary form. The particle size distribution depends on the process parameters. Fine particles give more transparent shades. The

finished pigment is sold by Clariant (which bought the pigment activities from Hoechst AG in 1997) as 'Hostaperm® Scarlet GO' and 'Hostaperm® Scarlet GO transparent'. The pigment is registered in the international Colour Index as 'CI Pigment Red 168' (PR 168).

PR 168 has an extremely high photostability; its light fastness and weather fastness are among the best of all the organic pigments. PR 168 is mainly used in coatings and paints (Herbst & Hunger, 2004). However, for coatings with full red shades, diketopyrrolopyrrole (DPP) pigments are preferred because they are cheaper than PR 168. However, if DPP pigments are applied in low concentrations, *e.g.* as a shading component or in pale pink coatings, the DPP dissolves in the coating media and causes a yellow fluorescence. In contrast, PR 168 remains undissolved and keeps its red shade even at very low concentrations. PR 168 is often combined with other pigments. For example, a combination of PR 168 with reddish–yellow pigments yields nice shades of bronze and copper, which are used for metallic car coatings.

To a lesser extent, PR 168 is used in plastics and printing inks.

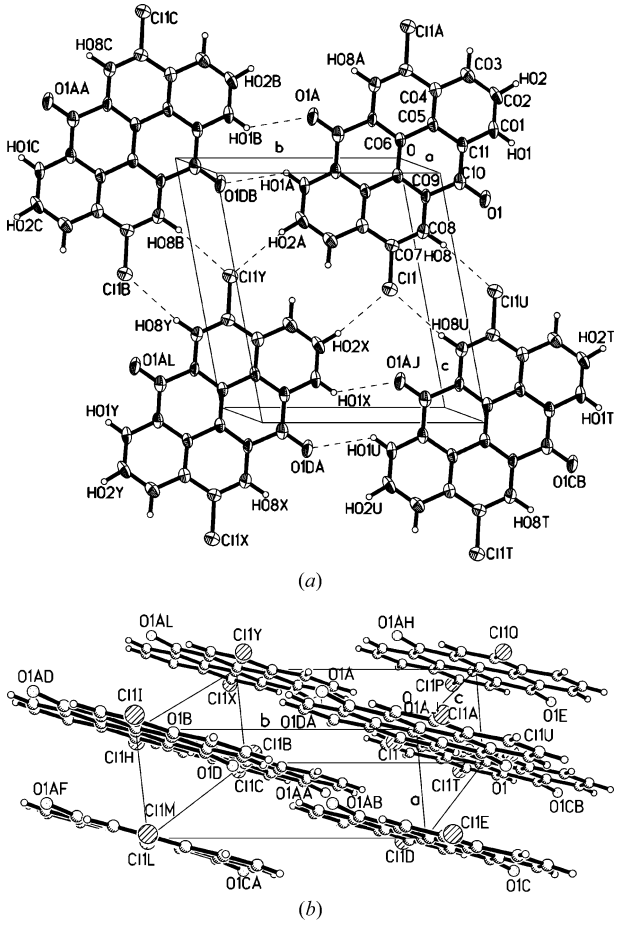

Figure 3
Crystal structure of 4,10-dichloro-anthanthrone (1). (*a*) Projection onto the (11$\bar{1}$) plane. Atomic nomenclature and atomic displacements (50% probability). Dashed lines indicate intermolecular Cl···H and O···H contacts. (*b*) View along the planes, view direction approximately [213].

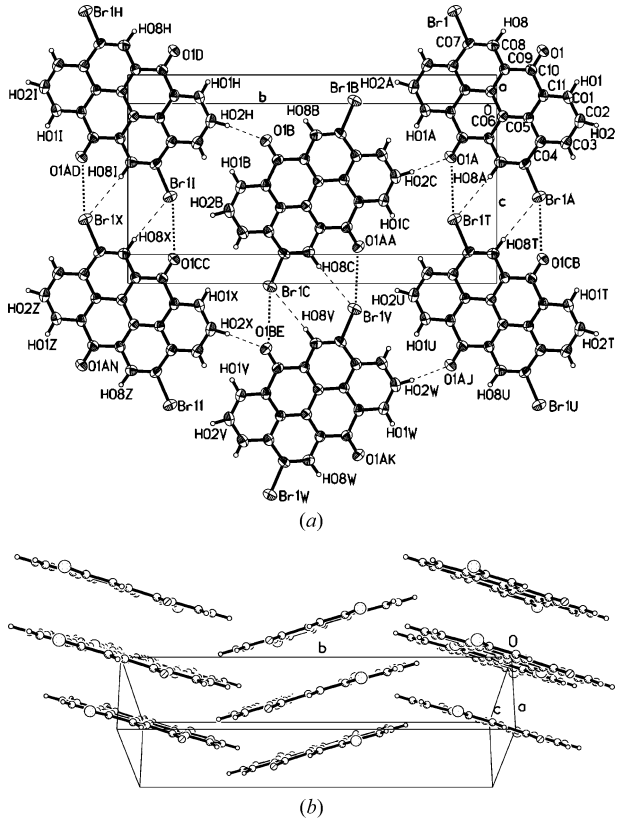

Figure 4
Crystal structure of 4,10-dibromo-anthanthrone, PR 168 (2). (*a*) Projection onto the (101) plane. Atomic nomenclature and atomic displacements (50% probability). Intermolecular Br···H and O···H contacts are shown as dashed lines; Br···O contacts are drawn as dotted lines. (*b*) View direction [10$\bar{1}$].

2. X-ray structure determinations

2.1. Crystallization and structure solution

Crystals of the dihalogenated anthanthrones were grown by dissolving the compounds in large quantities of *o*-dichlorobenzene at *ca* 443 K and cooling the solution to room temperature within a few days. Selected single crystals with the dimensions as shown in Table 1 were sealed in Lindemann glass capillaries, and single-crystal X-ray measurements were made on a Siemens R3m/V diffractometer with Mo $K\alpha$ radiation. In a relatively fast first run 25 strong reflections distributed over a 2θ range between 7 and 30° were selected to determine accurate cell parameters (Table 1). Absorption corrections were made by the ψ method (Kopfmann & Huber, 1968).

The structures were solved by direct methods using the program system *SHELXTL-Plus* (Sheldrick, 2008). Mo $K\alpha$ radiation has relatively large absorption effects for bromine compounds; nevertheless, for dibromo-anthanthrone the hydrogen positions could be determined from difference maps, and the isotropic displacement parameters for H atoms could be refined within reasonable ranges, as for the chloro

Table 2
Selected distances (Å) and other parameters (°, Å^3).

All values are calculated using idealized hydrogen positions with C—H distances of 1.08 Å.

	(I) X = Cl	(II) X = Br	(III) X = I
Intramolecular distances			
C—O	1.234 (5)	1.226 (4)	1.222 (7)
C—X	1.752 (4)	1.899 (3)	2.098 (5)
Intermolecular distances			
$X\cdots X$	3.795 (3)	3.865 (3)	4.202 (3)
$X\cdots$O	3.743 (4)	3.291 (4)	3.131 (4)
$X\cdots$H shortest	2.78 (1)	2.88 (1)	3.34 (1)
Second shortest	2.95 (1)	3.25 (1)	3.37 (1)
O$\cdots$H shortest	2.55 (1)	2.37 (1)	2.94 (1)
Second shortest	2.94 (1)	3.62 (1)	2.97 (1)
Intermolecular angles			
C—$X\cdots$O	162.0 (1)	159.6 (1)	167.5 (1)
C—$X\cdots$H shortest	124.6 (5)	112.6 (5)	135.4 (5)
Second shortest	125.6 (5)	148.5 (5)	123.9 (5)
C═O$\cdots$H shortest	133.0 (5)	129.8 (5)	133.7 (5)
Second shortest	110.6 (5)	95.5 (5)	104.0 (5)
Molecular planes			
Mean deviation out of molecular plane	0.032 (4)	0.037 (4)	0.017 (4)
Angles between molecular planes of neighboured stacks	0.0	0.0; 32.5 (4)	0.0; 14.1 (4)
Angle of molecular plane vector with a axis	26.3 (4)	28.0 (4)	33.9 (4)
Angle of molecular plane vector with b axis	74.1 (4)	73.7 (4)	82.9 (4)
Angle of molecular plane vector with c axis	23.7 (4)	70.4 (4)	46.5 (4)
Perpendicular distance of molecular planes in the stacks	3.402 (4)	3.414 (4)	3.486 (4)
Volume/molecule	368.0 (1)	379.3 (1)	401.4 (4)

compound. Atomic coordinates are given in Table S1 of the supplementary material.[1] The R values decrease in the order Cl > Br > I, which is probably an effect of the diffraction power of the halogen atoms and, maybe, of the crystal quality.

In order to ensure that the single crystal is indeed representative of the powder, the X-ray powder diagram of each compound was simulated and compared with the experimental powder diagram. The diagrams matched well. For dibromoanthanthrone the simulated diagram corresponds to the experimental diagram of the industrial product, Hostaperm® Scarlet GO.

No polymorphs have been described so far for (1)–(4).

2.2. Crystal structures

In all the crystal structures of anthanthrones, the molecules are planar. The most striking observation is that the bromine and iodine compounds have the same crystal symmetry ($P2_1/c$, Z = 2) and also quite similar lattice parameters (see Table 1). However, as concluded from the powder diffraction diagrams, the crystal structures are not the same, and this is proven by the single-crystal analyses.

The chlorine compound crystallizes in the triclinic space group $P\bar{1}$, Z = 1; the a and c cell constants are again similar to those before, except that the b axis is halved, and the number of molecules per unit cell is halved.

The crystal structures are shown in Figs. 3–5; selected distances and angles are given in Table 2.

For the interpretation of intermolecular distances it is difficult to choose the most appropriate van der Waals radii. For the drawings we have chosen the values which are suggested by the program system used (Sheldrick, 2008). For the discussion of intermolecular contacts, van der Waals radii are taken from Kitajgorodskij (1955) and Kitaigorodskii (1961). The values are: C 1.70, O 1.36, Cl 1.78, Br 1.95, I 2.1, H 1.18 Å. The most difficult problem is the value for hydrogen. Kitajgorodskij's value of 1.18 Å is based on a C—H distance of 1.08 Å. Consequently, for the discussion of intermolecular contacts and the comparison of different packings we will use idealized hydrogen positions, which have been calculated with C—H distances of 1.08 Å.

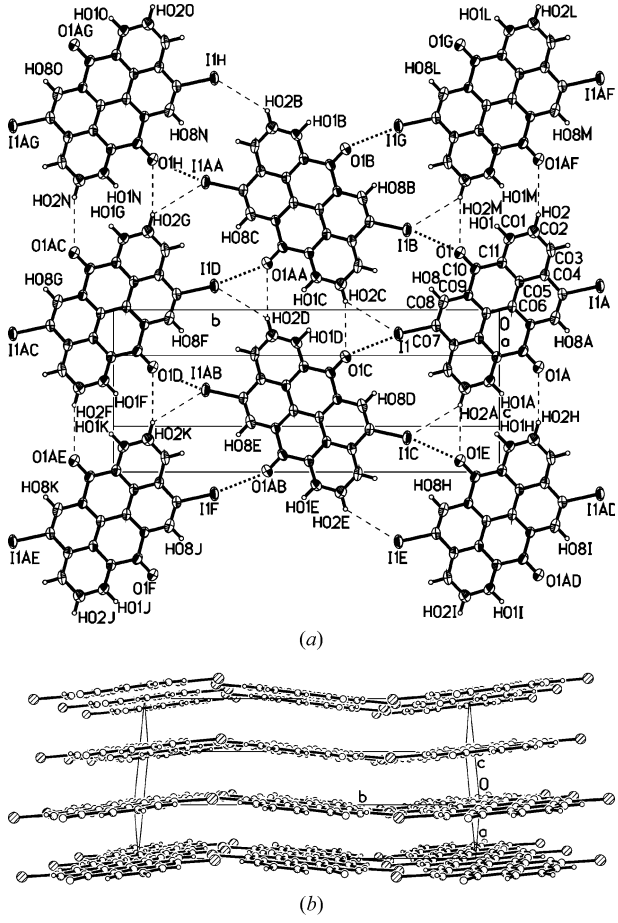

Figure 5
Crystal structure of 4,10-diiodo-anthanthrone (3). (*a*) Projection onto the (10$\bar{2}$) plane. Atomic nomenclature and atomic displacements (50% probability). Intermolecular I$\cdots$H and O$\cdots$H contacts are shown as dashed lines; I$\cdots$O contacts are drawn as dotted lines. (*b*) View direction [201].

[1] Supplementary data for this paper are available from the IUCr electronic archives (Reference: OG5041). Services for accessing these data are described at the back of the journal.

2.2.1. Dichloro-anthanthrone (1). Molecules of dichloro-anthanthrone form stacks along the crystallographic *a* axis. Within the stacks the distance between the molecular planes is 3.401 Å. When looking in projection onto the plane of the molecules, adjacent molecules within a stack are offset (shifted sidewards) by 1.7 Å in the direction parallel to the C═O bonds.

Between the stacks, there are short intermolecular Cl···H contacts (4 × 2.78 Å and 4 × 2.95 Å; sum of van der Waals radii: 2.96 Å, see Table 2); each stack is connected with four neighbouring stacks by two Cl···H contacts per molecule (Fig. 3*a*). The intermolecular halogen···oxygen distances (3.743 Å) are tremendously longer than in the other two crystal structures, although Cl atoms are smaller than Br and I atoms. The observed Cl···O distance is 0.6 Å larger than the sum of the van der Waals radii of Cl and O; *i.e.* the Cl···O interactions only have a minor influence on this packing.

There is also a very weak O···H interaction in the *b* direction (Fig. 3*a*, O1*A*···H01*B*: 2.55 Å), but its length even oversteps the van der Waals distance (2.54 Å).

All molecules are parallel, as reflected by the crystal symmetry ($P\bar{1}$, $Z = 1$). The normal vector of the molecular planes has an angle of 26.3° against the *a* axis. The molecular planes of neighbouring stacks are shifted with respect to each other in the *a* direction, leading to interplanar distances of 0.887 (molecule at $x + 1$, y, $z + 1$), 0.827 (molecule at $x + 1$, $y - 1$, z) and 1.714 Å (molecule at x, $y + 1$, $z + 1$), see Fig. 3(*b*).

2.2.2. Dibromo-anthanthrone [Pigment Red 168; (2)]. In dibromo-anthanthrone (2) the molecules form similar stacks as in the chlorine compound. The stacks run along the **a** direction (Fig. 4*a*). Within the stacks, neighbouring molecules are shifted by 1.8 Å in the direction of the C═O bonds, as in the dichloro derivative.

The molecules are planar; the average deviation of atoms out of the least-squares plane is only 0.037 Å. Molecules of stacks neighbouring in the **b** direction are not parallel, but are tilted relative to each other by 32.5°; both are tilted by 28.0° to the *a* axis (Fig. 4*b*).

The packing contains short contacts between the electronegative atoms bromine and oxygen (Fig. 4*b*). The Br···O distance of 3.291 Å is scarcely smaller than the sum of the van der Waals radii of 3.31 Å. A search of the Cambridge Structural Database (CSD; Cambridge Structural Database, 2009) shows that there are many organic structures with considerably shorter Br···O distances; the shortest distances are found if the angle C—Br···O is not far from 180° (here: 159.6°), because the van der Waals surface of a Br atom is not spherical, but shortened along the C—Br axis (see below). The Br···O distances of 3.291 Å observed for dibromo-anthanthrone indicate that it is not the Br···O interactions that mainly control the arrangement of the molecules in the crystal structure. The intermolecular Br1···H08 distance of 2.88 Å, however, is significantly smaller than the van der Waals sum of 3.13 Å. The intermolecular contact H02···O1 (2.37 Å) is also smaller than the van der Waals sum (2.54 Å) and could be considered as a weak hydrogen bond.

Other intermolecular distances (for example Br1···H02: 3.25 Å) are similar or larger than the van der Waals sums. Hence the packing of dibromo-anthanthrone can be regarded as a normal van der Waals packing of brick-shaped molecules, with a few non-negligible short intermolecular distances. Additionally there are weak Coulomb interactions caused by the non-uniform charge distribution within the molecules (H: slightly positive; O: negative; Br: in the C—Br direction less negative than in the perpendicular direction). As can be seen from Fig. 4(*a*) the molecules arrange in a way that these Coulomb interactions (Br···H, O···H) are favourable. However, detailed lattice-energy calculations are needed to judge whether it is these small electrostatic interactions which make the experimental structure more favourable than various other possible dense van der Waals packings (see §3).

2.2.3. Diiodo-anthanthrone (3). The lattice parameters and space group of diiodo-anthanthrone (3) are strikingly similar to those of dibromo-anthanthrone (2). At first glance, considering Figs. 4(*a*) and 5(*a*), the molecular arrangement also seems to be similar. However, the crystal structures are not actually isotypic, but do exhibit four major differences:

(i) The molecules are rotated around their normal axes by *ca* 60° (Figs. 4*a* and 5*a*).

(ii) Consequently, each molecule of the iodo compound now has I···O contacts with four different molecules in the plane, whereas the dibromo derivative has Br···O contacts to only two neighbouring molecules.

(iii) The layers in the diiodo structure are almost planar (tilting angle between neighbouring molecules 14.1°, see Fig. 5*b*), whereas in the dibromo derivative the layers are more wavy (tilting angle 32.5°).

(iv) Looking perpendicular to the molecules, the offset of neighbouring molecules is not parallel to the C═O bond (as in the dichloro and dibromo derivatives), but forms an angle of *ca* 54° with it.

Therefore, the similarity of lattice parameters and space groups of the iodo and bromo derivatives is only a coincidence, and not an indication of isotypy.

In the iodo compound the I···O distances of 3.131 Å are 0.16 Å shorter than in the bromine case, although the van der Waals radius of iodine is 0.15 Å larger than that of bromine. The I···O distances are 0.33 Å shorter than the sum of the van der Waals radii (3.46 Å). This short I···O contact becomes possible due to the non-sphericity of the iodine atoms (see §2.2.4).

In contrast, the I···H distances (3.34 Å; van der Waals sum: 3.3 Å) are not shortened to the same extent as in the bromine compound. The smallest intermolecular H···O distance, however, is quite long (O1*C*···H02*C*: 2.94; van der Waals sum: 2.54 Å). This means there is no C═O···H—C bridge. The much smaller angles between molecular planes of stacks neighboured in the *b* direction flatten the molecular sheets in the projection $(10\bar{2})$ much more than in the bromine compound in the (101) projection (Figs. 4*b* and 5*b*).

2.2.4. Effect of non-sphericity of the halogen atoms. Halogen atoms are known to be anisotropic (Nyburg & Faerman, 1985; Price *et al.*, 1994). Their shape as well as their

charge distribution is non-spherical. The halogen atom is shorter and more positive parallel to the C—*X* direction and more negative in the perpendicular directions. Consequently, neighbouring molecules prefer to arrange in a manner that atoms with negative partial charges (here: oxygen) approach parallel to the C—*X* bond, *i.e.* with C—*X*···O angles close to 180°, especially for chlorine, which is more electronegative than Br or I. On the other hand, atoms with positive partial charges (here: hydrogen) tend to lie perpendicular to the C—*X* bond, with C—*X*···H angles around 90°.

These arrangements can be found in all packings, irrespective of the halogen involved: The C—*X*···O angles are always around 180° and the C—*X*···H contacts are closer to 90° (see Table 3). Hence, this does not provide an explanation as to why (1), (2) and (3) adopt three different structures.

2.2.5. Unsubstituted anthanthrone (4). The crystal structure of the unsubstituted anthanthrone (4) was determined by Edwards & Stadler (1971). The structure is not isotypic to any of the dihalogenated compounds (1)–(3). The unsubstituted anthanthrone crystallizes in the space group $P2_1/c$ with the cell parameters $a = 20.9$, $b = 3.86$, $c = 33.2$ Å, $\beta = 92°$. The unit cell contains 8 molecules on three different sites: four molecules are on a general position (Wyckoff position 4*e*), two molecules on inversion centres at (0,0,0) and $(0, \frac{1}{2}, \frac{1}{2})$ (site 2*a*), and two on further inversion centres at $(\frac{1}{2}, 0, \frac{1}{2})$ and $(\frac{1}{2}, \frac{1}{2}, 0)$ (site 2*d*), see Fig. 6(*a*). According to the notation of Zorkij (Chernikova *et al.*, 1990), the corresponding structural class is denoted as $P2_1/c$, $Z = 8$ ($\bar{1}_a$,$\bar{1}_d$,1). This crystal symmetry is very rare (Chernikova *et al.*, 1990; Belsky *et al.*, 1995).

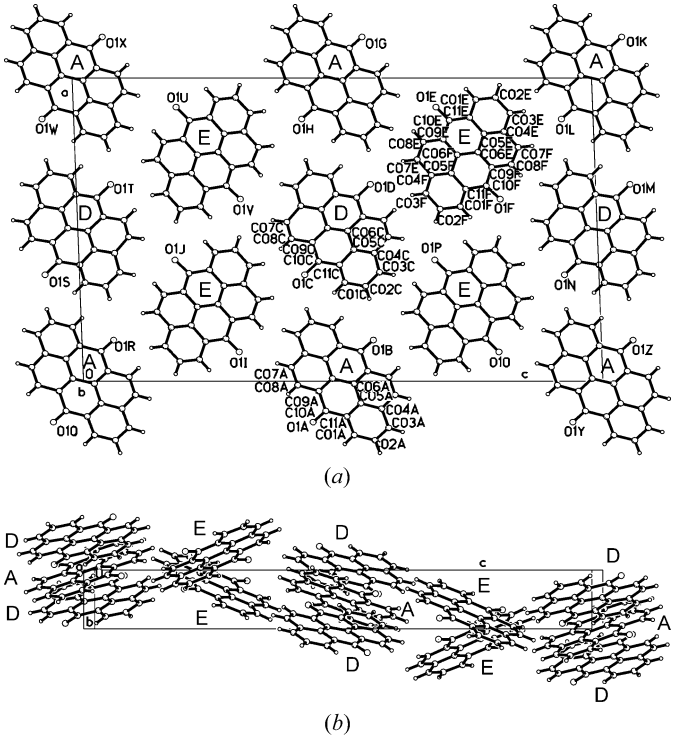

Figure 6
Crystal structure of the unsubstituted anthanthrone (4). Space group $P2_1/c$, $Z = 8$. The three symmetrically independent molecules are denoted with *A*, *D* and *E*. Molecules *A* and *D* are situated on crystallographic inversion centres at Wyckoff positions 2*a* and 2*d*, whereas molecules *E* are on a general position (Wyckoff position 4*e*). (*a*) View direction [010] and atomic nomenclature. (*b*) Projection onto the (100) plane.

The crystal structure is shown in Fig. 6. The molecules form stacks along the crystallographic *b* axis. The interplanar spacings in the stacks are 3.464, 3.503 and 3.547 Å, which is not at all smaller than in the halogenated compounds (3.402, 3.414 and 3.486 Å), *i.e.* the halogen atoms do not lead to an increase in the interplanar distances. The molecules of (4) are inclined against the stack direction by 24.8, 23.2 and 26.2°. Looking perpendicular to the planes of the individual molecules, adjacent molecules within a stack of molecules at Wyckoff positions 2*d* are shifted in the direction of the C═O bond (as in the dichloro and diiodo derivative), whereas molecules at sites 2*a* and 4*e* are shifted perpendicular to the C═O bond.

The interplanar angles between the molecules are 4.1, 33.7 and 35.4°. A view along the *a* axis (Fig. 6*b*) shows that the molecular packing is a combination of parallel packing (as in the chloro derivative) and herringbone packing (as in the bromo compound). Each of these packing motifs is frequently observed for planar aromatic compounds, but it is very unusual to find both motifs combined in the same crystal.

In the unsubstituted anthanthrone, there are intermolecular O···H distances between 2.5 and 2.6 Å which are practically equal to van der Waals distances, *i.e.* there is no special C═O···H—C interaction dominating the crystal packing.

2.2.6. Comparison of the structures; discussion. The four anthanthrones (1)–(4) form four different structures. Although the lattice parameters of the bromo and iodo derivatives are quite similar, the molecular packings are clearly different. All molecules (1)–(4) are arranged in parallel stacks, like most planar aromatic molecules. As frequently observed for such compounds, the stacks of (1)–(4) form hexagonal rod packings. Molecules of stacks adjacent in the **b** direction are parallel for the chloro compound, inclined for the bromo compound slightly inclined for the iodo derivative; whereas the unsubstituted derivative shows a combination of parallel and inclined arrangements (here in the **c** direction).

The reason for the formation of four different packings remains obscure. There is no common 'synthon' (*e.g.* halogen···halogen interactions) which is responsible for the packings. In contrast, most halogen···halogen distances as well as the halogen···oxygen, halogen···hydrogen and oxygen···hydrogen distances are – with a few differences – equal or larger than the van der Waals distances; moreover, they vary from compound to compound, not following any visible trend. Thus, the 'synthon' approach fails to explain the structural differences.

All four packings are dominated by van der Waals interactions, which depend on the molecular shape. Correspondingly all packings can be considered as brick packings. At least for the bromo compound, however, the weak hydrogen bridges cannot be fully neglected. Nevertheless, since molecules differ only in the size of the substituent *X* (*X* = H, Cl, Br, I) we would expect the formation of only one or two different packings, *e.g.* one packing for small substituents, the other packing for larger substituents. Hence, the van der Waals

approach as well as the geometrical approach fails to explain the structural differences. The weak intermolecular Coulomb interactions seem to play a decisive role in determining which of the possible dense van der Waals packings are energetically most favourable.

3. Lattice-energy calculations

Lattice-energy calculations were performed in order to understand the differences in crystal packing of the four molecules.

For each of the anthanthrone derivatives (X = H, Cl, Br, I), the structures and energies of four crystal structures were calculated: that of the observed crystal structure and three hypothetical structures derived from the crystal structures of the three analogues. We refer to the four packing alternatives as (I), (II), (III) and (IV) for the molecules (1) (X = Cl), (2) (X = Br), (3) (X = I) and (4) (X = H).

3.1. Computational details

Idealized molecular geometries were derived by optimization of the isolated molecule at the MP2/3-21G level of theory (using the program *CADPAC*; Amos, 1995) and these were constrained to be rigid in all further calculations. These optimized molecular structures of each derivative were placed in each crystal structure (aligning all C and O atoms) as starting points for the lattice-energy calculations and the 16 resulting crystal structures were lattice-energy minimized using anisotropic atom–atom model potentials. For comparison, lattice-energy calculations were also performed using the semi-classical density sums (SCDS-Pixel) approach (Gavezzotti, 2003*a*,*b*).

Owing to the importance of anisotropy in atom–atom repulsion involving halogen atoms (Nyburg & Faerman, 1985; Price *et al.*, 1994), the traditional spherical-atom description is not appropriate for these molecules. We therefore used an exp-6 model with anisotropy incorporated into the exponential description of the repulsion

$$U_{\text{repulsion-dispersion}} = \sum_{i,k} \left[A^{\iota\kappa} \exp(-B^{\iota\kappa}[R_{ik} - \rho^{\iota\kappa}(\Omega_{ik})]) - C_6^{\iota\kappa} R_{ik}^6\right], \quad (1)$$

where $A^{\iota\kappa}$, $B^{\iota\kappa}$ and $C^{\iota\kappa}$ are the parameters describing interactions between atoms i and k of type ι and κ.

The function $\rho(\Omega_{ik})$ describes the relative orientation of the atoms and is defined by the atomic z axes ($\boldsymbol{z}_i$, $\boldsymbol{z}_k$) and the interatomic vector, $\boldsymbol{R}_{ik}$, with z axes for all carbon, hydrogen and halogen atoms defined along the C—X bonds (X = H, O, Cl, Br, I), pointing out from the molecule. C atoms not at the periphery of the molecule were treated as spherical

$$\rho^{\iota\kappa}(\Omega_{ik}) = \rho_1^{\iota}(\mathbf{z}_i \cdot \mathbf{R}_{ik}) + \rho_1^{\kappa}(-\mathbf{z}_i \cdot \mathbf{R}_{ik}) + \rho_2^{\iota}\left(3[\mathbf{z}_i \cdot \mathbf{R}_{ik}]^2 - 1\right)/2 + \rho_2^{\kappa}\left(3[\mathbf{z}_k \cdot \mathbf{R}_{ik}]^2 - 1\right)/2. \quad (2)$$

All parameters (A, B, C, ρ_1, ρ_2) for interactions involving only chlorine, carbon and hydrogen were taken from the non-empirical potential derived for chlorobenzenes (Day & Price, 2003). I···I, O···O, I···O, I···H and O···H parameters were taken from the potential derived for use in the recent blind test of crystal structure prediction (Day's entry in Day *et al.*, 2005).

Parameters for all atom types are given in the supplementary material. Parameters for interactions involving bromine were fitted specifically for this work, in the same way as those used for iodine interactions (Day *et al.*, 2005), by adjusting the parameters to minimize the change in geometry (unit-cell parameters and molecular positions in the unit cell) on lattice-energy minimization of the crystal structures of 1,5-dibromonaphthalene (Haltiwanger *et al.*, 1984; CSD refcode COXLOQ) and 2,3,6,7-tetrabromonaphthalene (Singh *et al.*, 1980; CSD refcode BRNPHL). During parameterization, the anisotropy parameter of the repulsion (ρ_2, with ρ_1 = 0) was fixed to give the anisotropy observed by Nyburg & Faerman (1985) (we refer to this parameter set as model 1). Application of this parameter set led to an unexpected energy ranking (see below), which prompted us to investigate two further parameter sets in the atom–atom calculations. Calculations were performed using two models based on Price's model potential derived for the brominated molecule in the second blind test of crystal structure prediction (Motherwell *et al.*, 2002). The first of these models (model 2) used the Br···Br and Br···X (X = C, H, O) parameters taken directly from Price's work, while the third model (model 3) took Br···Br parameters from Price and Br···X parameters from geometric combining rules with the C···C, H···H and O···O parameters derived for the other two (chloro and iodo) halo-anthanthrones. The electrostatic interactions between molecules were modelled by a distributed multipole analysis of the MP2/3-21G calculated charge density, placing multipoles up to hexadecapole on each atom. All lattice-energy calculations using these anisotropic potentials were performed with the crystal structure modelling program *DMAREL* (Price *et al.*, 2001).

SCDS-Pixel calculations were performed using the *OPiX* program (Gavezzotti, 2003*c*), using the most recent scheme for treating repulsion interactions (Gavezzotti, 2005). The SCDS-Pixel calculations were performed with the same MP2/3-21G calculated charge density (recalculated using the program *GAUSSIAN*03 (Frisch *et al.*, 2004), as was used for the electrostatics in the atom–atom potential. Structure type (IV) with three independent molecules had to be omitted from the SCDS-Pixel calculations, as the version of the *OPiX* software used in this work is restricted to $Z' \leq 1$ crystal structures.

Owing to the lack of analytical energy derivatives in the SCDS-Pixel method, the structure optimization is less efficient so the crystals were optimized with *DMAREL* first (using a modified Newton–Raphson algorithm), then with SCDS-Pixel (using a Simplex algorithm), starting from the *DMAREL* final structure. 15 Å cutoffs, based on molecular centres of mass, were used in all (atom–atom and SCDS-Pixel) calculations, except charge–charge, charge–dipole and dipole–dipole interactions in *DMAREL*, which were treated using Ewald summation.

Table 3
Lattice energies (kJ mol^{-1}) of the observed (indicated by an asterisk) and hypothetical crystal structures of the unsubstituted and halogenated anthanthrones.

The lowest energy structure for each molecule is highlighted in bold.

Halogen	Method	Structure type (I)	(II)	(III)	(IV)
Chloro	Atom–atom	−175.2*	**−175.7**	−167.2	−167.0
	SCDS-Pixel	**−152.1***	−150.9	−140.2	–
Bromo	Atom–atom model 1	**−180.0**	−177.4*	−179.8	−174.5
	Atom–atom model 2	−155.8	−152.6*	**−156.0**	−150.6
	Atom–atom model 3	**−155.5**	−151.6*	**−155.5**	−150.2
	SCDS-Pixel	**−137.4**	−133.4*	−135.2	–
Iodo	Atom–atom	−163.1	−158.7	**−166.7***	−156.9
	SCDS-Pixel	−148.9	−147.8	**−151.3***	–
Unsubstituted	Atom–atom	−147.0	−141.8	−148.5	**−154.9***
	SCDS-Pixel	−148.8	−140.3	**−150.0**	–

3.2. Results

After energy minimization, the four observed crystal structures are reproduced very well (see supplementary information for a comparison of the lattice-energy-minimized and observed crystal structures). From the atom–atom calculations, cell lengths in the energy-minimized crystal structures of the bromo (model 1) and iodo compounds are all within 2% of the observed cell lengths, while maximum deviations in cell lengths increase to about 4% for the crystal structures of the chloro and unsubstituted anthanthrones, as well as for the bromo molecule with the 'model 2' and 'model 3' potential parameters. R.m.s. errors in the lengths of *a*, *b* and *c* are 2.93, 3.40, 1.13, 0.66% for unsubstituted, dichloro-, dibromo- (model 1) and diiodo-anthanthrones. R.m.s. errors in the lengths of *a*, *b* and *c* are slightly larger after energy minimization with SCDS-Pixel (3.26, 5.18 and 1.59% for the chloro, bromo and iodo molecules).

The magnitudes of the calculated lattice energies vary significantly between methods (Table 3), but the relative energies of the four crystal structures for each molecule are reasonably constant (Fig. 7).

With both approaches to calculating the lattice energies, the observed structure of the iodo compound is significantly more stable than the alternative hypothetical structures, by more than 2.4 kJ mol^{-1} (atom–atom calculations) or 3.6 kJ mol^{-1} (SCDS-Pixel). The order of stability for the iodo compound is (III) > (I) > (II) with both methods of calculating lattice energies, and the atom–atom calculations place structure (IV) even higher in energy. In fact, structure (IV) is the least stable of the four packings for all three halogenated anthanthrones and does not seem to be an energetically feasible polymorph for any of these molecules. Structure (IV) is, on the other hand, much more stable (by over 6 kJ mol^{-1}) than the other three crystal structures for the unsubstituted anthanthrone. The observed crystal structures of the iodo and unsubstituted anthanthrones are the most stable of the possibilities examined in this work.

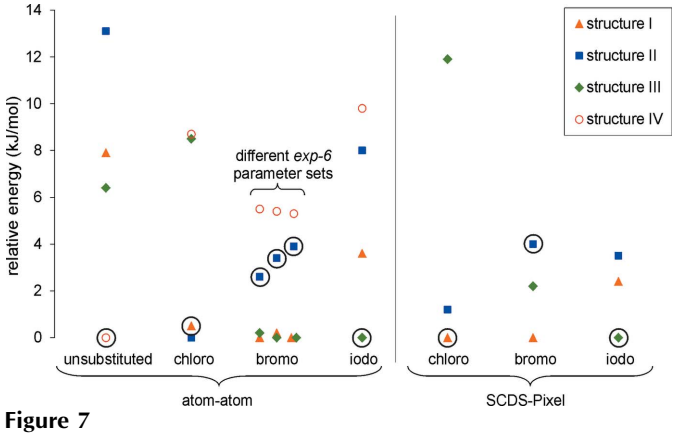

Figure 7
Calculated relative lattice energies of the observed and hypothetical crystal structures of the unsubstituted and 4,10-dihalogenated anthanthrones. Experimental structure types are marked with large circles.

Results of the lattice-energy calculations for the chloro derivative are less clear-cut; both methods find structure (II) very close in energy to the observed structure [type (I)]. The atom–atom calculations place structure (II) at slightly lower energy (0.5 kJ mol^{-1}) than structure (I), but this is well within the limits of static lattice-energy minimization, *i.e.* ignoring all but the internal energy contribution to free energy differences. The SCDS-Pixel calculations place the observed structure [type (I)] lower in energy than any others [1.2 kJ mol^{-1} lower in energy than structure (II)]. Structures (III) and (IV) are significantly (> 8 kJ mol^{-1}) less stable than the observed crystal.

Our results for the dibromo anthanthrone are the most interesting; the observed crystal structure [type (II)] is consistently calculated to be higher in energy than both structures (I) and (III), for all applied parameter sets in the atom–atom calculations. While the magnitude of lattice energies varies from model to model (Table 3), all three atom–atom parameter sets give nearly the same relative energies – the hypothetical structures (I) and (III) are almost equienergetic and 3–4 kJ mol^{-1} more stable than the observed crystal. The SCDS-Pixel calculations give a similar picture, with structure (I) of the brominated molecule the most stable.

Agreement between all models indicates that other polymorphs of 4,10-dibromo-anthanthrone could exist, which are isotypic to the dichloro- or the diiodo derivatives, and that one of these hitherto unknown polymorphs might even be more stable than the known crystal structure. The discovery of such latent polymorphism of industrially important molecules is becoming more common as computational and experimental investigations are combined (Day *et al.*, 2006).

4. Searching for the missing polymorphs of dibromo-anthanthrone

Surprisingly, the polymorphism of dibromo-anthanthrone seems to have never been investigated, although the pigment has been industrially produced for more than 80 years. This is even more remarkable because it has been known for decades that the crystal structure of organic pigments has a strong

effect on their colouristic properties (such as hue, shade and colour strength), on the crystal morphology and on the stabilities (photostability, fastness to weathering, fastness to migration in plastics). For example, the γ-phase of quinacridone [(7), see Fig. 8] is red, the β phase is a reddish violet; both β- and γ-phases are industrially used in coatings. In contrast, the isolated molecule is yellow, *i.e.* the red and violet colours are caused only by the molecular packing (Paulus *et al.*, 2007).

For indanthrone (8), which has a similar molecular shape to dibromo-anthanthrone, four polymorphic forms are known. From the investigations of the British intelligence office and the corresponding US authorities in Germany after the second world war, we know that these polymorphic forms were investigated by X-ray powder diffraction at the BASF company as early as in 1934 (BIOS report, 1946;[2] FIAT report, 1948; see also Kunz, 1939), which was only 18 years after the first X-ray powder diagrams were made by Debye & Scherrer (1916) and Hull (1917).

4.1. Polymorph screening and X-ray powder diffraction

Is there another polymorph of dibromo-anthanthrone which is isostructural to the dichloro or diiodo derivative, as indicated by the lattice-energy calculations?

Indeed, after the computational study, described in §3, was completed, we recognized that there is a second, metastable polymorph. This β-polymorph is formed upon synthesis and sold under the tradename 'Indanthrene Brilliant Orange RK®'. Finishing, *e.g.* by recrystallization from sulfuric acid, leads to the more stable α-phase which is described above.

A comparison of the powder diagram of the β-phase with the simulated diagrams of the predicted structures clearly shows that the β-phase does not correspond to one of the hypothetical structures investigated here, *i.e.* the β-phase is not isostructural to the dichloro or diiodo derivatives (see Fig. 9).

In order to search for further polymorphs of dibromo-anthanthrone, we attempted to perform a full polymorph screening using various recrystallization methods. However, the experiments were hampered by the fact that the compound is definitively insoluble in water and all solvents, even at temperatures above 473 K. Even boiling 'exotic' solvents did not help, *e.g.* morpholene (b.p. 401 K), picolene (b.p. 402 K), 2-ethyl-1-hexanole (b.p. 457 K), *N*-methylpyrrolidone (b.p. 475 K) or quinolene (b.p. 511 K). Stirring the pigment as a suspension under these conditions did not change the polymorphic form. Melting (at temperatures far above 573 K) results in decomposition. Sublimation is possible at 473 K in high vacuum, but results only in the formation of the poorly crystalline α-phase. The pigment can be 'dissolved' by treatment with concentrated acids, *e.g.* concentrated sulfuric acid or trifluoroacetic acid; in these media the pigment is protonated and forms a green solution. Upon dilution, *e.g.* with 80% H_2SO_4, the pigment precipitates as a powder in the α- or β-phase. Similar results were obtained when the pigment is reduced in an alkaline sulfite solution and subsequently re-oxidized.

However, we cannot rule out that, *e.g.* by using other synthetic routes, a metastable third polymorph could be formed, which indeed is isotypic to the dichloro or diiodo derivatives, as predicted by the lattice-energy minimizations.

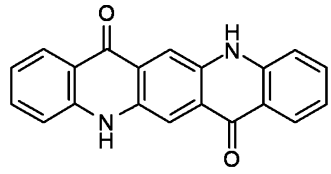

Quinacridone (7)

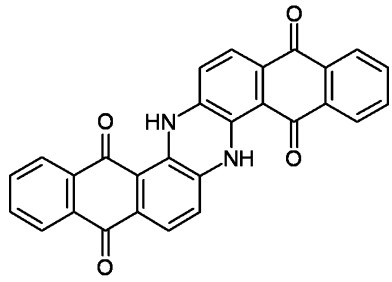

Indanthrone (8)

Figure 8
Molecular formula of quinacridone (7) and indanthrone (8).

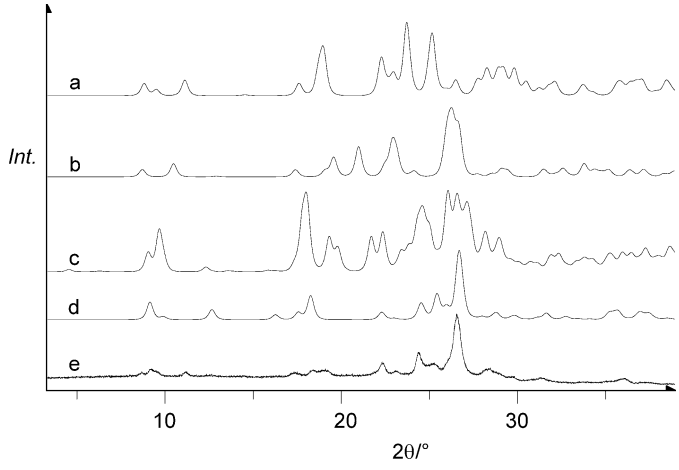

Figure 9
Searching for the missing polymorph of dibromo-anthanthrone. Simulated X-ray powder diagrams of different predicted crystal structures. From the top: (*a*) packing of dibromo-anthanthrone like dichloro-anthanthrone, (*b*) like diiodo-anthanthrone, (*c*) like unsubstituted anthanthrone; (*d*) calculated diagram of the α-phase of dibromo-anthanthrone, (*e*) experimental X-ray powder diagram of the β-phase of dibromo-anthanthrone. It can be seen that the β-phase does not correspond to any of the simulated structures, *i.e.* the β-phase of dibromo-anthanthrone is not isostructural to any of the other derivatives.

[2] The BIOS report contains a translation of an unpublished report on the application of the X-ray technique in the chemical industry by Dr Georg von Susich of Wilhelmsfeld near Heidelberg relating to the work of von Susich at the IG laboratories in Ludwigshafen.

4.2. Attempts to solve the crystal structure of the β-phase of dibromo-anthanthrone by crystal-structure prediction

The β-phase is a nanocrystalline powder. Single crystals cannot be grown. All experimental attempts to improve the crystallinity of the β-phase failed: either the crystallinity did not change or the pigment transformed into the more stable α-phase. The X-ray powder diagrams always consist of only a few broad lines. The best powder diagram ever obtained is shown in Fig. 9 (bottom). The diagram was recorded in transmission mode on a Stoe-Stadi-P diffractometer equipped with a Ge(111) monochromator and a linear position-sensitive detector, using Cu $K\alpha_1$ radiation. The large peak widths are caused by the low crystallinity of the sample, not by the diffractometer.

None of the powder diagrams of the β-phase could be indexed in a reliable way. Therefore, we attempted to solve the crystal structure by crystal structure prediction. This approach has been successfully applied, *e.g.* on the dioxazine pigment $C_{22}H_{12}Cl_2N_6O_4$ using a powder diagram consisting of 12 lines (Schmidt *et al.*, 2005).

Possible crystal structures of dibromo-anthanthrone were predicted by force-field methods using the program *CRYSCA* (Schmidt & Kalkhof, 1999).

The intermolecular energy was calculated using the Dreiding/X6 force field (Mayo *et al.*, 1990) with atomic charges calculated by the method of Gasteiger & Marsili (1980). The calculations started from a large set of randomly generated structures, having random values (within user-defined ranges) for lattice parameters, molecular orientations and positions (if not on $\bar{1}$). The molecules were treated as rigid.

The molecular geometry was taken from the *ab initio* calculations, as in §3.

Dibromo-anthanthrone has molecular symmetry 2/*m*. The CSD shows that 95% of all molecules with 2/*m* symmetry are located on crystallographic inversion centres, whereas other site symmetries are rarely occupied (Pidcock *et al.*, 2003). The most frequent space groups for molecules with 2/*m* symmetry are $P\bar{1}$ ($Z = 1$), $P2_1/c$ ($Z = 2$), $C2/c$ ($Z = 4$) and $Pbca$ ($Z = 4$), each with molecules on inversion centres. Correspondingly the crystal structure predictions were performed with those crystal symmetries. The calculations were run in the corresponding subgroups ($P1$, Pc, $C2$ and $P2_12_12_1$) with complete molecules on fixed positions. Additional calculations were performed with molecules on general positions in space groups which are generally frequent for aromatic compounds, including $P\bar{1}$ ($Z = 2$) and $P2_1/c$ ($Z = 4$). Most of the resulting structures showed additional symmetry and could be transformed to the corresponding higher-symmetrical space groups (supergroups). By this approach, a large variety of crystal symmetries is covered, including structures with molecules on mirror planes (*e.g.* $P2_1/m$, $Z = 2$ or $Pnma$, $Z = 4$) or on twofold axes (*e.g.* $C2/c$, $Z = 4$).

All low-energy minima (excluding duplicates) were post-optimized with the three anisotropic atom–atom potentials described in §3. The equivalent structures to the known dichloro and diiodo derivatives are found in the list of predicted structures, and are amongst the lowest energies with all three model potentials. The structure of the α-phase has a higher energy, as described in §3.

In order to determine which of the predicted structures corresponds to the β-phase, X-ray powder diagrams were calculated for all low-energy structures and compared with the experimental powder diagram of the β-phase. However, it turned out that there were at least four structures which had an X-ray powder similar to the experimental one (Figs. 10*a* and *b*). These structures differ considerably from each other in space groups, lattice parameters and packing motifs, including herringbone, criss-cross and double-herringbone packings (Figs. 10*c*–*e*). Obviously, the quality of the experimental data is not sufficient to select the correct structure. Rietveld refinements would not help because for data of this quality even the refinement of the wrong crystal structure could give a good Rietveld fit (Buchsbaum & Schmidt, 2007). Hence, the crystal structure of the β-phase of dibromo-anthanthrone remains undetermined.

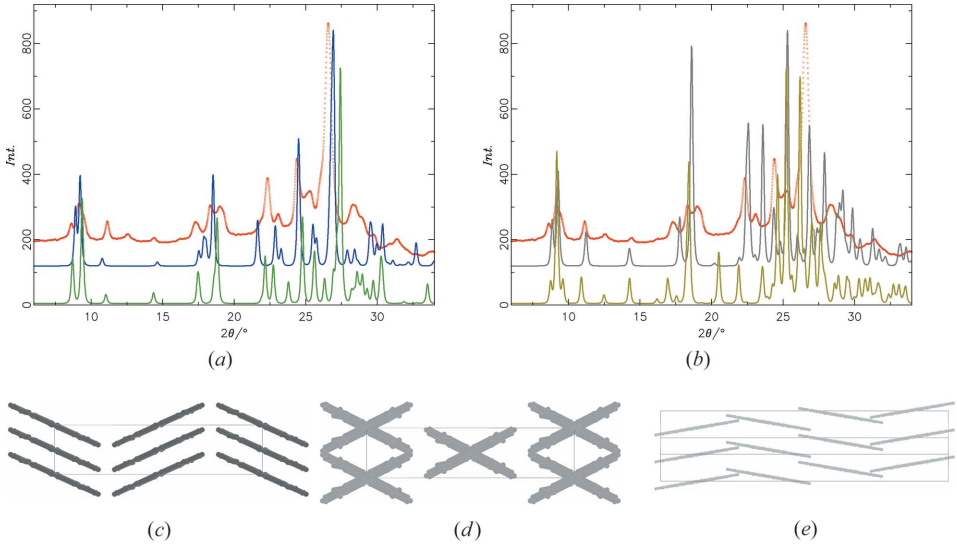

Figure 10
Attempts to solve the crystal structure of β-(2) by crystal structure prediction: (*a*) Simulated powder diagrams of the predicted structures *A* (middle) and *B* (bottom). Top: Experimental powder diagram. (*b*) Simulated powder diagrams of the predicted structures *C* (middle) and *D* (bottom). Top: Experimental powder diagram. (*c*) Structure *A*, space group $C2/c$, $Z = 4$, (*d*) structure *B*, space group $C2/c$, $Z = 4$, (*e*) structure *D*, space group $P2_1/c$, $Z = 4$. The powder diagrams are similar, although the packings are different. Owing to the low crystallinity of β-(2), it is not possible to determine which of the predicted structures corresponds to the experimental one.

5. Conclusion

The four molecules studied here crystallize in four different crystal structures, despite their molecular similarity. For three compounds [(1), (3) and (4)] lattice-energy calculations show that each molecule crystallizes in its energetically most favourable crystal structure. For the fourth compound, dibromo-anthanthrone (2), the calculations predicted the molecule to crystallize isotypically to the dichloro or diiodo derivative. Crystallization experiments have failed to yield either of these alternative structures, but lead to the detection of a metastable polymorph. Owing to the very low crystallinity of this polymorph, its crystal structure could not be determined, but it is certainly different from all of the four other structures.

The authors thank Dr Arpad Acs and his group (formerly at Hoechst AG, now Clariant, Frankfurt) for syntheses, and Winfried Heyse and Harald Schweizer (both formerly at Hoechst AG, now Sanofi-Aventis, Frankfurt) for crystallizations. Sublimations were carried out by the group of Dr Karl-Heinz Schweikart (Clariant, Frankfurt). X-ray powder diffractograms were measured by Ursula Conrad (formerly at Hoechst AG, Frankfurt) and Edith Alig (Goethe-University Frankfurt). We thank Dr Dieter Schnaitmann, Dr Wolfgang Hoyer (both Clariant, Frankfurt) and Dr Werner Spielmann (Allessa, Frankfurt) for samples and information about PR 168. The financial support of Clariant is gratefully acknowledged.

References

Amos, R. D. (1995). *CADPAC*, Version 6.0. University of Cambridge, England.
Belsky, V. K., Zorkaya, O. N. & Zorky, P. M. (1995). *Acta Cryst.* A**51**, 473–481.
BIOS report (1946). *German Organic Pigments and Lake Dyestuffs.* British Intelligence Objectives Sub-committee. HM Stationary Office. Technical information and documents unit, London 1946 (Investigations 24 July to 23 August 1946), pp. 412–463.
Bradley, W. & Waller, J. (1953). *J. Chem. Soc.* pp. 3783–3786.
Buchsbaum, C. & Schmidt, M. U. (2007). *Acta Cryst.* B**63**, 926–932.
Cambridge Structural Database (2009). Cambridge Crystallographic Data Centre, 12 Union Road, Cambridge, England.
Chernikova, N. Yu., Bel'ski, V. K. & Zorkij, P. M. (1990). *Zh. Strukt. Khim.* **31**, 148–153.
Day, G. M. *et al.* (2005). *Acta Cryst.* B**61**, 511–527.
Day, G. M. & Price, S. L. (2003). *J. Am. Chem. Soc.* **125**, 16434–16443.
Day, G. M., Trask, A. V., Motherwell, W. D. S. & Jones, W. (2006). *Chem. Commun.* pp. 54–56.
Debye, P. & Scherrer, P. (1916). *Phys. Zeit.* **17**, 277–283.
Edwards, I. A. S. & Stadler, H. P. (1971). *Acta Cryst.* B**27**, 946–952.
FIAT report (1948). Final Report No. 1313, *German Dyestuffs and Dyestuff Intermediates, Including Manufacturing Processes, Plant Design, and Research Data*, Vol. 3: Dyestuff research, prepared by Field Information Agency, Technical (FIAT), United States Group Control Council for Germany.
Fieser, L. F. & Fieser, M. (1957). *Lehrbuch der organischen Chemie*, p. 1069. Weinheim: Verlag Chemie.
Formánek, J. & Knop, J. (1927). *Untersuchung und Nachweis organischer Farbstoffe auf spektroskopischem Wege*, Vol. 2, Teil 4. Berlin: Julius Springer-Verlag.
Frisch, M. J. *et al.* (2004). *GAUSSIAN*03, Revision D.01, Gaussian, Inc., Wallingford, CT, USA.
Gasteiger, J. & Marsili, M. (1980). *Tetrahedron*, **36**, 3219–3222.
Gavezzotti, A. (2003*a*). *CrystEngComm*, **5**, 429–438.
Gavezzotti, A. (2003*b*). *CrystEngComm*, **5**, 439–446.
Gavezzotti, A. (2003*c*). *OPiX*. University of Milano, Italy.
Gavezzotti, A. (2005). *Z. Kristallogr.* **220**, 499–510.
Haltiwanger, R. C., Beurskens, P. T., Vankan, J. M. J. & Veeman, W. S. (1984). *J. Crystallogr. Spectrosc. Res.* **14**, 589–597.
Herbst, W. & Hunger, K. (2004). *Industrial Organic Pigments*, 3rd ed. Weinheim: Wiley-VCh.
Herz, R. & Zerweck, W (1932). Patent US 1877315.
Hull, A. W. (1917). *Phys. Rev.* **10**, 661–696.
Kalb, L. (1913*a*). Deutsches Reichspatent 280787.
Kalb, L. (1913*b*). *Deutsches Reichspatent* 287250.
Kalb, L. (1914). *Ber. Dtsch. Chem. Ges.* **47**, 1724–1730.
Kitajgorodskij, A. I. (1955). *Organicheskaya Kristallokhimiya*. Moskva: Iso-vo Akad. Nauk SSSR.
Kitaigoroskii, A. I. (1961). *Organic Chemical Crystallography*. New York: Consultants Bureau.
Kopfmann, G. & Huber, R. (1968). *Acta Cryst.* A**24**, 348–351.
Kunz, M. (1939). *Angew. Chem.* **52**, 269–282.
Maki, T. & Hashimoto, H. (1953). *Bull. Chem. Soc. Jpn*, **26**, 348–351.
Mayo, S. L., Olafson, B. D. & Goddard, W. A. III (1990). *J. Phys. Chem.* **94**, 8897–8909.
Motherwell, W. D. S. *et al.* (2002). *Acta Cryst.* B**58**, 647–661.
Mix (1986). Internal report of Cassella AG, Frankfurt am Main.
Nyburg, S. C. & Faerman, C. H. (1985). *Acta Cryst.* B**41**, 274–279.
Paulus, E. F., Leusen, F. J. J. & Schmidt, M. U. (2007). *CrystEngComm*, **9**, 131–143.
Pidcock, E., Motherwell, W. D. S. & Cole, J. C. (2003). *Acta Cryst.* B**59**, 634–640.
Price, S. L., Willock, D. J., Leslie, M. & Day, G. M. (2001). *DMAREL*, Version 3.1. University College London.
Price, S. L., Stone, A. J., Lucas, J., Rowland, R. S. & Thornley, A. E. (1994). *J. Am. Chem. Soc.* **116**, 4910–4918.
Schaeffer, A. (1951). *Die Entwicklung der künstlichen organischen Farbstoffe.* Hofheim-Marxheim.
Schmidt, M. U., Ermrich, M. & Dinnebier, R. E. (2005). *Acta Cryst.* B**61**, 37–45.
Schmidt, M. U. & Kalkhof, H. (1999). *CRYSCA*. Frankfurt am Main, Germany.
Schultz, G. (1934). *Farbstofftabellen*, 7th ed. Auflage, Ergänzungsband I. Leipzig: Akademische Verlagsgesellschaft m.b.H.
Schweizer, H. R. (1964). *Künstliche organische Farbstoffe und ihre Zwischenprodukte*, p. 374. Berlin, Göttingen, Heidelberg: Springer-Verlag.
Sheldrick, G. M. (2008). *Acta Cryst.* A**64**, 112–122.
Siemens (1989). *R3m/V Software*. Siemens Analytical Instruments Inc., Madison, Wisconsin, USA.
Singh, P., McKinney, J. D. & Levy, L. A. (1980). *Cryst. Struct. Commun.* **9**, 563–566.